Title. Influence of Accelerated Ageing on the Physico-mechanical Properties of Alkali Treated Industrial Hemp Fibre Reinforced Polylactic Acid (PLA) Composites.

M.S.Islam[1*], K.L.Pickering[1] and N.J.Foreman[2]

[1]Department of Engineering, The University of Waikato, Private Bag 3105, Hamilton, New Zealand

[2]Hemptech, PO Box 46033, Herne Bay, Auckland, New Zealand.

Abstract. In this study, 30 wt% aligned untreated long hemp fibre/PLA (AUL) and aligned alkali treated long hemp fibre/PLA (AAL) composites were produced by film stacking and subjected to accelerated ageing environment. Accelerated ageing was carried out with an accelerated ageing chamber using UV-irradiation and water spray at 50 °C for four different time intervals (250, 500, 750 and 1000 hrs). After accelerated ageing, tensile strength (TS), flexural strength, Young's modulus (YM), flexural modulus and mode I fracture toughness (K_{Ic}) were found to decrease and impact strength (IS) was found to increase for both AUL and AAL composites. AUL composites had greatest overall reduction in mechanical properties than that for AAL composites upon exposure to accelerated ageing environment. FTIR analysis and crystallinity contents of the accelerated aged composites support the results of the deterioration of mechanical properties upon exposure to accelerated ageing environment.

Keywords. Hemp Fibre, Polylactic Acid, Accelerated Ageing, Impact Strength, Fracture Toughness.

1. Introduction

Natural fibres such as hemp, flax, jute and kenaf have received considerable attention as an environmentally friendly alternative for the use of glass fibres in polymer composites [1]. They exhibit excellent mechanical properties especially when their low density and price are taken into account [2, 3]. They have high strength and modulus to weight ratios, fatigue and corrosion resistant. However, because of their unknown long term

*To whom correspondence should be addressed (Current address: CSIRO Materials Science and Engineering - Geelong, Henry Street, Belmont 3216, Victoria, Australia, Cell: +61413345047, E-mail: Saiful.Islam@csiro.au).

properties when exposed to a combination of in-service loads and environments, designers are still reluctant to use natural fibre composites in primary load bearing structures [4]. The effect of exposure to moisture, heat, and ultra-violet (UV) radiation, and more importantly a combination of these parameters may degrade the material's stiffness and strength.

Durability of natural fibre composites upon exposure to UV-light is of particular concern as UV-light can cause the changes in the surface chemistry of the composites commonly known as photodegradation [5, 6]. The degradation ranges from mere surface discoloration affecting the aesthetic appeal in indoor applications to extensive loss of mechanical properties [7, 8]. Moreover, the combination of light, moisture, and temperature in outdoor applications can completely destroy the lignocellulosic network, limiting the performance of unprotected wood in outdoor applications[9]. The photodegradation of natural fibres like wood is attributed to the degradation of its components namely cellulose, hemicelluloses, and lignin according to Dence [10]. Lignin and hemicelluloses are more prone to degradation than cellulose by various means [11]. Lignin degrades upon exposure to UV-light and hemicelluloses degrade upon moisture absorption and biological means [12]. The UV-degradation process is known to be triggered by the formation of free radicals and probably starts with the oxidation of phenolic -hydroxyls [13]. Moreover, singlet oxygen that can be formed by oxygen quenching of photoexcited lignin plays a role in the degradation of lignocellulosic natural fibres like wood [13]. The formed singlet oxygen is a source of peroxides [14], which can initiate the auto-oxidation of carbohydrates and cleavage of lignin [15, 16]. In polylactic acid (PLA) matrix the active oxygen species initiate the degradation reaction by attacking neighbouring PLA chain and the degradation process extends into the PLA through the diffusion of these reactive oxygen species [17].

Ideally, composite materials and their structures that are intended for long term use should be tested in real time and with realistic in-service environments. Often this is not viable because the time involved would significantly delay product development and therefore, accelerated ageing techniques are required [4]. During accelerated weathering, measured variables can include exposure time, exposure to UV irradiation over a specific wavelength range, and exposure to moisture as number of cycles or time. Therefore, the purpose of this work was to produce aligned untreated long hemp fibre/PLA (AUL) and aligned alkali treated long hemp fibre/PLA (AAL) composites to observe the influence of accelerated ageing on the mechanical and physical properties of the composites.

2. Experimental

2.1 Materials

Retted bast hemp fibre (TS of about 526 MPa and 32.6 μm) was supplied by Hemcore, UK. Film grade PLA (Tarde mark of 4042D, density of 1.25 g/cm^3) in the form of pellets, was obtained from Nature Works, USA. Analytical grade Na_2SO_3, and 98% NaOH pellets were used for the alkali treatment of fibres.

2.2 Methods

2.2.1 Treatment of the Fibres with Alkali

Unwanted pieces of woody core were manually removed from the retted bast hemp fibre. After weighing, fibres were placed into stainless steel canisters of 1L capacity. Pre-weighed NaOH and Na_2SO_3 solution was then poured into the canisters such that the fibre to 2 wt% Na_2SO_3 and 5 wt% NaOH solution ratio was 1:2:10 by weight. The canisters were then placed into a small lab-scale pulp digester at 120^{o}C for 60 minutes. Fibres were then washed in a pulp and paper fibre washer for about 45 minutes to remove chemical residues until a fibre pH of about 7 was obtained. Fibres were then dried in an oven for 48 hours at 70^{o}C.

2.2.2 Production of Preform Fibre Mats

For the production of hemp fibre/PLA composites, long untreated and alkali treated fibres were dried at 80^{o}C for 24 hrs. Aligned long fibre mats were produced by aligning 60g of fibres using a hand carding machine from Ashford Handicrafts Limited, Ashburton, New Zealand to obtain a mat thickness of 3.5 mm.

2.2.3 Fabrication of Composites.

PLA pellets were micronised into PLA powder using a microniser. PLA powder was then used to produce PLA sheets of 3 mm thickness using a hot press at 170^{o}C and 1 MPa pressure maintained for 5 minutes. A fibre mat was then sandwiched between two PLA films in a preheated compression mould (commonly known as film stacking). This was then pressed at a temperature of 170^{o}C and a pressure of about 1 MPa for 10 minutes to produce AUL and AAL Composites of 30 wt% fibre content.

2.2.4 Composite Mechanical Testing

Composite mats were cut into tensile, flexural, impact, and fracture toughness test specimens using a band saw according to the specified standard test methods for each of

the tests as described below. Five to six replicates were used for each test. The samples were then placed in a conditioning chamber at 23°C ± 3°C and 50% ± 5% relative humidity for 40 hours. Tensile testing was carried out in accordance with ASTM D 638-03 Standard Test Method for Tensile Properties of Plastics. The specimens were then tested using an Instron-4204 tensile testing machine fitted with a 5 kN load cell at a rate of 1 mm/min. An Instron 2630-112 extensometer was used to measure strain. Flexural (three point bend) testing was carried out in accordance with the ASTM D 790-03 Standard Test Methods for Flexural Properties of Unreinforced and Reinforced Plastics and Electrical Insulating Materials using a Lloyd LR 100 K tensile testing machine fitted with a 5 kN load cell. Charpy impact testing was carried out in accordance with the International Standard Organization (ISO) 179 Standard Test Method. Dimensions of the samples were 80 mm × 8 mm × 4 mm with a single notch of 0.25 mm (type A). An advanced universal pendulum impact tester POLYTEST with an impact velocity of 2.9 m/s and a hammer weight of 0.475 kg at 21°C was used. Single-edge-notch bend (SENB) specimens were obtained in accordance with ASTM D 5045-99 Standard Test Methods for Plane-Strain Fracture Toughness and Strain Energy Release Rate of Plastic Materials. The specimens were then tested using a Lloyd LR 100 K tensile testing machine fitted with a 5 kN load cell operating at a rate of 10 mm/min to obtain mode I (tensile mode) fracture toughness or plain strain fracture toughness (K_{Ic})

2.2.5 Optical and Scanning Electron Microscopy.

An optical microscope (Olympus BX 60) was used to assess composite surface porosity and major crack of fracture toughness specimens with a calibrated eyepiece at 200× magnification. The fracture surfaces of the composites were examined using a Hitachi S-4000 Field Emission SEM operated at 5 kV. Carbon tape was used to mount the samples on aluminum stubs. The samples were then sputter coated with platinum and palladium to make them conductive prior to scanning electron microscopic observation.

2.2.6 Differential Scanning Calorimetry (DSC) Analysis.

DSC analysis was carried out using a DSC 2920 differential scanning calorimeter, in an argon atmosphere with a heating rate of 5°C/min. A static argon flow of 50 mL/min and an aluminum sample pan were used. Specimens of approximately 10 mg were scanned over a temperature range of 25 to 200°C. The glass transition temperature (T_g), melt temperature (T_m), cold crystallization temperature (T_c), and heat of melting (ΔH_m) were determined for each of the neat PLA and composite samples. Details of cold crystallization and pre-melt crystallization can be found in the literature [18, 19]. The percentage crystallinity of each sample was calculated using the relationship

$$X_c(\%Crystallinity) = \frac{\Delta H_m}{\Delta H_m^0} \times \frac{100}{w} \quad (1)$$

where ΔH_m is the heat of melting, ΔH_m^0 is the heat of melting for 100% crystalline PLA sample (taken as ΔH_m^0 = 93 J/g) and w is the weight fraction of PLA in the sample [20, 21]. To determine the crystallinity of the sample, the heats of cold crystallization and pre-melt crystallization were subtracted from heat of melting [22].

2.2.7 Wide Angle X-ray Diffraction (WAXRD) Analysis

WAXRD analysis of neat PLA, untreated and alkali treated fibres (fibres were formed into tablets using hydraulic press), AUL and AAL Fibre/PLA film stacked composites was carried out using a Philips X-ray diffractometer, employing CuKα (λ = 1.54) radiation and a graphite monochromator with a current of 40 mA and a voltage of 40 mV was used with a diffraction intensity in the range of 6 to 60o (2θ-angle range).

2.2.8 Fourier Transform Infrared (FTIR) Spectra

The FTIR spectra analysis of the composites was carried out using an FTIR Digilab FTS-40 spectrometer. Untreated and alkali treated fibres were ground into small particles in liquid nitrogen and mixed and compressed with potassium bromide (KBr) into a thin disc using a hydraulic press at 8 MPa pressure.

2.2.9 Accelerated Ageing of the Composites

Accelerated ageing of the samples was carried out using an accelerated weathering tester (Model QUV/spray with solar eye irradiance control) in accordance with ASTM G 154-00a: Standard Practice for Operating Fluorescence Light Apparatus for UV Exposure of Non-metallic Materials. A fluorescent bulb (UVA) with 0.68 W/m^2 irradiance (at 340 nm) was used with cycles of 1 hour UV irradiation, followed by 1 minute of spray with de-ionized water and a subsequent 2 hours condensation while maintaining a temperature of 50^{o}C. Five specimens from each batch of tensile, flexural, impact, and fracture toughness testing samples were subjected to the ageing process for durations of 250, 500, 750, and 1000 hours.

3. Results and discussion

3.1. Accelerated Ageing

As can be seen from Figure 1, the exposure of the samples to accelerated ageing environments slightly deteriorated the surface texture in the form of decoloration, appearance of a milky colour on the surface, and surface softness. The yellowish colour of the samples after accelerated ageing might be due to the breakdown of the lignin into

water soluble products [13, 23].

The aged surface showed an accentuation of fibres with the erosion of PLA, Figures 2(a) and 2(b). The appearance of milky patches, matrix cracks, and swollen fibres are more severe for AUL composites than that for AAL composites. The deterioration of the composites is likely to be initiated by the fibre ridging followed by PLA film rupture through cracking and then fibre pop-out. This is attributed mainly to the stresses produced by differential swelling and shrinkage of the fibre/PLA caused by changes in moisture content. Stresses also built up at the fibre/matrix interface due to a large difference between the coefficients of thermal expansion for PLA matrix and hemp fibre, leading to the failure of the fibre/PLA interface [24]. Increasing exposure to the weathering conditions led to the initiation of tearing in the fibres is more likely to be due to degradation by UV attack.

Progressive percentage weight gain in the samples during accelerated ageing is shown in Figure 3. It can be seen that percentage weight gain for neat PLA was lower than that for the composites. Weight gain for AAL composites was higher than for AUL composites after accelerated ageing for 250 hours and weight gain for AUL composites were higher after accelerated ageing for 500 and 750 hours. The weight gain for composites was found to be reduced and weight loss for PLA was found to occur after accelerated ageing for 1000 hours. The weight gain for both neat PLA and composites might be caused by the absorption of water during water spray and condensation cycles. The low amount of moisture absorbed by neat PLA is expected due to its hydrophobic nature and the high amount of moisture absorbed by the composites is more likely to be due to the hydrophilic nature of the fibres by the presence of polar groups such as –OH and –COOH in the fibres. The higher water absorption by AAL composites after accelerated ageing of 250 hours may be due to increased hydrophilicity of alkali treated fibres [25] and the lower absorption of water after accelerated ageing of 500 and 750 hours may be due to the formation of stronger interfacial bonding between alkali treated fibre and PLA matrix upon removal of surface impurities such as hemicelluloses. The weight loss of PLA and decrease in weight gain for the composites after accelerated ageing of 1000 hours might be caused by leaching out of the PLA upon exposure to the ageing environment.

3.2. Effect of Accelerated Ageing on Mechanical Properties

The change in mechanical properties due to accelerated ageing for different time periods is presented in Figures 4 to 6. A reduction in tensile strength (TS), flexural strength,

Young's modulus (YM), and flexural modulus from their mean values for neat PLA and composites with increased ageing duration was observed (Figures 4 and 5). However, as shown in the figures 4 and 5 neat PLA was not tested after accelerated ageing of 1000 hours as it was too soft to be tested.

The greatest overall reduction in TS, flexural strength, YM, and flexural modulus was observed for AUL composites than for AAL composites. Tensile and flexural strengths were found to decrease from 61 and 115 MPa to 8 and 13 MPa respectively while, YM and flexural modulus were found to decrease from 8 and 6 GPa to 1 and 2 GPa respectively for AUL composites (Figures 4 and 5). However, TS, flexural strength, YM and flexural modulus were found to reduce for AAL composites than for AUL composites after accelerated ageing of 250 hours and after that (for 500, 750 and 1000 hours) they were found to reduce more for AUL composites than for AAL composites. Impact strength (IS) was found to increase dramatically for all of the composites after 250 hours of accelerated ageing with a continued increase up to 750 hours and a decrease after this time. IS of neat PLA was found to decrease with increased accelerated ageing time (Figure 6(a)). K_{Ic} was found to decrease for all samples with increased weathering time, with greatest decrease from 3.2 to 0.6 MPa.m$^{1/2}$ found for AUL composites (Figure 6(b)).

The reduction in TS, flexural strength, YM, and flexural modulus for neat PLA with increased duration of accelerated ageing is considered to be due to plasticisation, swelling effect [26] and photochemical degradation [27]. Although weight loss of neat PLA by photodegradation and leaching out would be expected to decrease the molecular weight of neat PLA leading to increase of crystallinity and as a consequence a reduction in YM, the plasticization effect in the neat PLA chains by moisture absorption could really increase the toughness which could outweigh the effect of increased crystallinity of neat PLA and hence a resultant decrease of YM. The reduction in TS, flexural strength, YM, and flexural modulus of the composites might be due to the development of swelling stresses, caused by the difference of expansion and contraction of fibre/PLA as a result of moisture absorption [24]. . The higher reduction in TS, flexural strength, YM, and flexural modulus of AAL composites after accelerated ageing of 250 hours may be due to increased hydrophilicity of alkali treated fibres [25] and the lower reduction in TS, flexural strength, YM, and flexural modulus after accelerated ageing of 500, 750 and 1000 hours may be due to the formation of stronger interfacial bonding between alkali treated fibre and PLA matrix as discussed previously. Stronger bond formation could reduce wicking of the moisture and penetration of UV-radiation into

the composites which may lead to less reduction in structural integrity for AAL composites than for AAL composites (Figure 7(a) and 7(b)). Also, as alkali treatment of fibres reduced relative amount of lignin [28], therefore, it is very likely that AUL composites would be less susceptible to UV-radiation and as a result more retention of mechanical properties than for AUL composites. Fibrillation of the fibres in the composite fracture surfaces was also noticed (Figures 7(a) and 7(b)) showing degradation of lignin which acts as an adhesive holding cellulose fibrils together. After lignin degradation, the poorly bonded cellulose fibrils could erode easily from the surface, which could expose new lignin embedded cellulose fibrils for subsequent degradation reaction and thus would be expected to enhance fibre pull-out from PLA. Thus more loss of structural integrity can be seen for AUL composite (Figure 7(a)) than for AAL composite (Figure 7(b)). The ageing process could make the composite surface rougher and also could lead to significant fibre loss from the surface according to other researchers [29].

PLA is a semicrystalline polymer and the degree of crystallinity of the processed PLA was found to be about 22%. As crystalline regions are impermeable to oxygen, degradation can occur predominantly in the amorphous regions by chain scission, while UV-induced cross-linking can occur in the imperfect crystalline regions. The reduction IS and K_{Ic} of neat PLA with weathering of up to 750 hours could be due to PLA chain scission and formation of surface cracks, which can be seen in Figure 8. After weathering of 1000 hours, softening and leaching of PLA made the samples too soft to be tested. The increase in IS and decrease in K_{Ic} for the composites may be due to the formation of porous structure as a result of leaching of debonded fibres by the fibrillation process upon removal of lignin. As a result of the increase in porosity, more water molecules would be expected to be trapped inside the composite structure, which may have a plasticising effect, resulting in the increase in IS and decrease in K_{Ic} [27]. Swelling of fibres as a result of water absorption also could cause the fibres to be pulled-out of the PLA matrix, increasing energy dissipation which in turn might increase the IS and decrease the K_{Ic} of the composites. The decrease IS of the composites after 1000 hours of weathering might be caused by failure of PLA by softening and leaching out. AAL composites showed better overall resistance to accelerated weathering due to the formation of stronger fibre/PLA bonds as discussed previously.

3.3. Fourier Transform Infrared (FTIR) Spectra Analysis

Analyses of the FTIR spectra of AUL composites (Figure 9) shows an increase in the

intensity of the C=O absorption for the 1000 hours weathered sample over the control sample in the 1734 cm^{-1} region and also around 1600 cm^{-1} [30]. The increase in the carbonyl absorption indicates modification in the lignin structure. The increase in the intensity of the 1600 cm^{-1} band may indicate quinine formation by irradiation during accelerated ageing which was found at around 1650 cm^{-1} region by other researchers [30]. The bands at 1734 and 1600 cm^{-1} are characteristic absorptions of carbonyl stretching vibrations of non-conjugated (in xylan) and conjugated (in lignin) esters and carboxylic acids, and their concentration increases as carbonyl groups are liberated from lignin and/or carbohydrates due to chemical degradation [30-32]. Pure PLA has a C-H deformation band at 1350 to 1460 cm^{-1}, which was found to be at 1400 cm^{-1} for both control and accelerated aged samples[17].

3.4. Wide Angle X-ray Diffraction (WAXRD) Analysis

Figure 10 shows the WAXRD patterns for AUL and AAL composites after 1000 hours accelerated ageing. PLA shows a narrow and sharp peak at $2\theta = 16.4$, which is attributed to the crystalline nature of the PLA. The peak intensity increased tremendously for the accelerated aged samples showing the increase in crystallinity of PLA after accelerated ageing. The sharp peak at $2\theta = 22.5$ for the crystalline cellulose was found to decrease significantly for the aged composites, showing a decrease in cellulose crystallinity due to the degradation of cellulose upon accelerated ageing. The intensity drop for the peak at $2\theta = 22.5$ was found to be greater for the AUL composites when compared to AAL composites, indicating a higher degradation of cellulose for the AUL composites upon accelerated ageing.

3.5 Differential Scanning Calorimetry (DSC) Analysis

Figure 11 shows the DSC traces for AUL and AAL composites after accelerated ageing of 1000 hours. The glass transition temperature was found to decrease from about 61^{o}C to about 42 and 45^{o}C, and melt temperature was found to decrease from about 148^{o}C, to about 140 and 144^{o}C for AUL and AAL composites respectively. The depression of the glass transition and melt temperature by photodegradation of PLA has also been observed by other researchers [17, 33]. The shoulder in the endothermic melting peak was found to disappear for AAL composite while the shoulder was found to merge for AUL composite after accelerated aging of 1000 hours. However, the degree of crystallinity was found to increase from about 26 to 38% for AUL composite while for AAL composite it was found to increase from about 31 to 45%. The increase in crystallinity could be caused by the rearrangement of the amorphous PLA segments into crystalline phase during the degradation of PLA by chain scission. This process is

known as chemicrystallisation [34]. The increase in crystallinity of PP upon UV exposure by the chemicrystallisation process and segmental mobility of the amorphous region has been reported by other researchers [27].

4. Conclusion

After accelerated ageing, TS, flexural strength, YM, flexural modulus and K_{Ic} were found to decrease and IS was found to increase for both AUL and AAL composites. AUL composites were found to be more resistant after 250 hours of accelerated ageing whereas AAL composites were found to be more resistant after 500 to 1000 hours of accelerated ageing. However, AUL composites had greatest overall reduction in mechanical properties than that for AAL composites. Results obtained from FTIR analysis and crystallinity contents of the accelerated aged composites also indicated the deterioration of mechanical properties upon exposure to accelerated ageing environment.

5. References

1. Peijs T, Melick HGH, Garkhail SK, Pott GT and Baille CA. Proceedings of the European Conference on Composite Materials: Science, Technologies and Applications, ECCM-8, 1998, pp 119-126.
2. Rowell RM. Proceedings of a seminar, Copenhagen, Denmark, 1995, pp 27-41.
3. Gassan J and Bledzki AK, Polymer Composites 1997;18: 179-184.
4. Martin R and Campion R, Materials World 1996;4: 200-202.
5. Stark NM and Matuana LM, Journal of Applied Polymer Science 2003;90: 2609-2617.
6. Matuana LM, Kamdem DP and Zhang J, Journal of Applied Polymer Science 2001;80: 1943-1950.
7. Kiguchi M and Evans PD, Polymer Degradation and Stability 1998;61: 33-45.
8. Matuana LM and Kamdem DP, Polymer Engineering Science 2002;42: 1657-1666.
9. Muller U, Ratzsch M, Schwanninger M, Steiner M and Zobl H, Journal of Photochemistry and Photobiology B: Biology 2003;69: 97-105.
10. Dence CW, The determination of lignin. Springer-Verlag, 1992.
11. Harper S, Composites 1982;13: 123-138.
12. Anglesa MN, Ferrandob F, Farriola X andSalvadoa J, Biomass and Bioenergy

2001;21: 211-224.
13. Hon DNS, Weathering and photochemistry of wood. New York: Marcel Dekker, 2000.
14. Beckert W and Lauke B, Composites Science and Technology 1997;57: 1689-1706.
15. Schmidt J, Kimura F and Gray DG, Res. Chem. Intermed 1995;21: 287-301.
16. Argyropoulus DS, Heitner C and Schmidt JA, Res. Chem. Intermed 1995;9: 263-274.
17. Nakayama N and Hayashi T, Polymer Degradation and Stability 2007;92: 1255-1264.
18. Wunderlich B, The Journal of Chemical Physics 1958;29: 1395-1404.
19. Ljungberg N and Wesslen B, Biomacromolecules 2005;6: 1789-1796.
20. Reinsch VE and Kelley SS, Journal of Applied Polymer Science 1997;64: 1785.
21. Vasanthakumari R and Pennings A, Polymer 1983;24: 175.
22. Nam JY, Ray SS and Okamoto M, Macromolecules 2003;36: 7126.
23. Heitner C, Light induced yellowing of wood containing papers. American Chemical Society, 1993.
24. Devis Aand Sims D, Weathering of plastics. UK: Applied Science Publishers, 1983.
25. Islam MS, Pickering KL and Foreman NJ, In press of Journal of Adhesion Science and Technology 2009:
26. Chen Y, Davalos JF, Ray I and Kim HY, Composite Structures 2007;78: 101-111.
27. Joseph PV, Rabello MS, Mattoso LHC, Joseph K and Thomas S, Composite Science and Technology 2002;62: 1357-1372.
28. Islam MS, Pickering KL and Foreman NJ, In press of Journal of Applied Polymer Science 2009:
29. Singh B, Gupta M and Verma A, Composites Science and Technology 2000;60: 581-589.
30. Pandey KKand Chandrashekar N, Journal of Applied Polymer Science 2006;99: 2367-2374.
31. Pandey KK, Journal of Applied Polymer Science 1999;71: 1969.

32. Harrington KJ, Higgins HG andMichell AJ, Holzforschung 1964;18: 108.
33. Copinet A, Bertrand C, Longieras A, Coma V and Couturier Y, Journal of Polymers and the Environment 2003;11: 169-179.
34. Pyda M, Bopp RC and Wunderlich B, J.Chem.Thermodynamics 2004;36: 731-742.

Figure Number and Caption to the Figures

Figure 1 Visual change during ageing of AUL and AAL composites.
Figure 2 (a) AUL and (b) AAL composite surfaces after 1000 hours accelerated ageing.
Figure 3 Percentage weight gain of neat PLA, AUL and AAL composites.
Figure 4 Effect of accelerated ageing on the (a) TS and (b) YM of neat PLA, AUL and AAL composites. Each error bar corresponds to one standard deviation.
Figure 5 Effect of accelerated ageing on (a) flexural strength and (b) flexural modulus of neat PLA, AUL and AAL composites. Each error bar corresponds to one standard deviation.
Figure 6 Effect of accelerated ageing on (a) IS and (b) K_{Ic} of neat PLA, AUL and AAL composites. Each error bar corresponds to one standard deviation.
Figure 7 (a) AUL and (b) AAL composite fracture surfaces after 1000 hours accelerated ageing.
Figure 8 SEM micrograph of neat PLA surface after weathering for 750 hours.
Figure 9 FTIR spectra of AUL composites.
Figure 10 WAXRD pattern for (a) AUL and (b) AAL composites before and after accelerated ageing of 1000 hours.
Figure 11 DSC traces for (a) AUL and (b) AAL composites before and after accelerated ageing of 1000 hours.

Figure 1 Visual change during ageing of AUL and AAL composites.

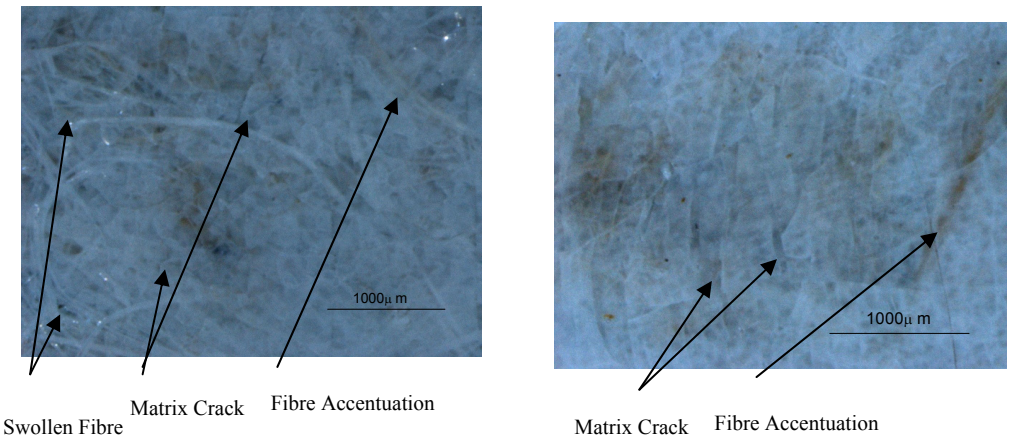

(a) **(b)**

Figure 2 (a) AUL and (b) AAL composite surfaces after 1000 hours accelerated ageing.

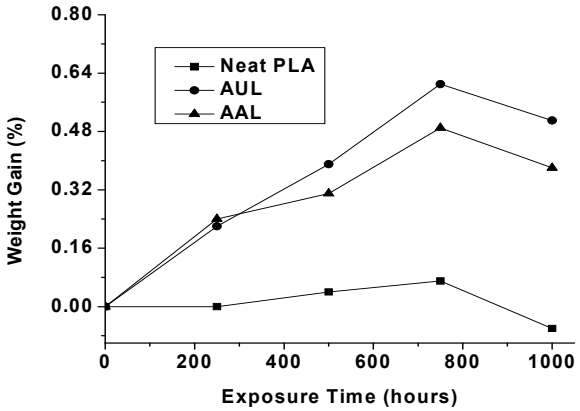

Figure 3 Percentage weight gain of neat PLA, AUL and AAL composites.

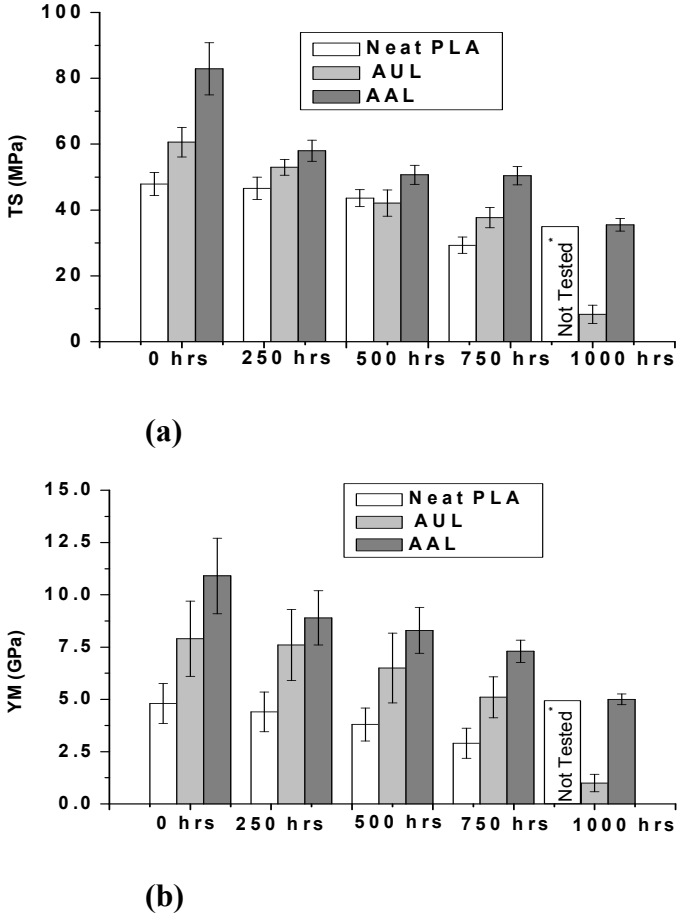

Figure 4 Effect of accelerated ageing on the (a) TS and (b) YM of neat PLA, AUL and AAL composites. Error bars each corresponds to one standard deviation.

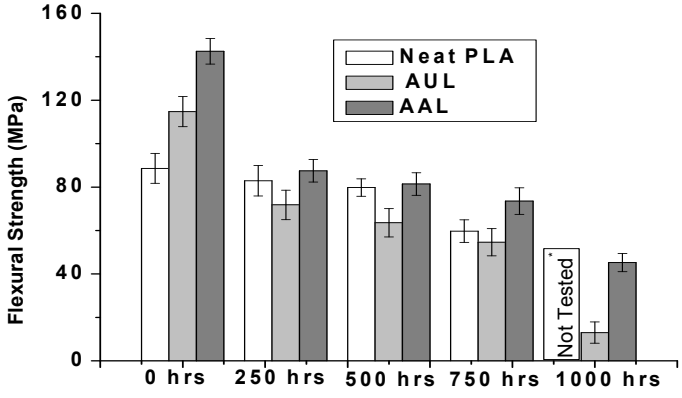

(a)

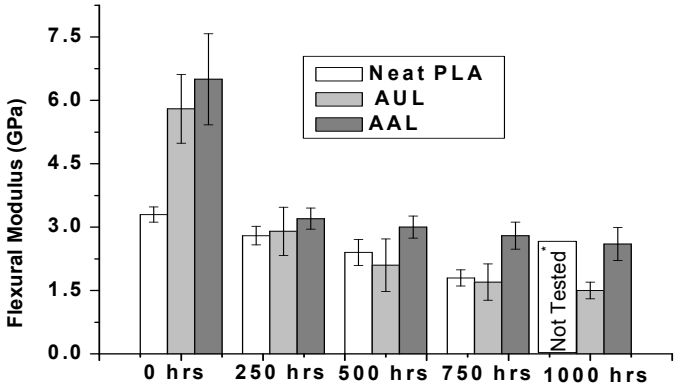

(b)

Figure 5 Effect of accelerated ageing on (a) flexural strength and (b) flexural modulus of neat PLA, AUL and AAL composites. Error bars each corresponds to one standard deviation.

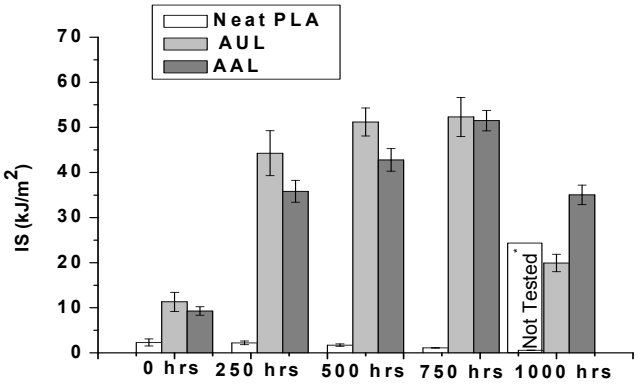

(a)

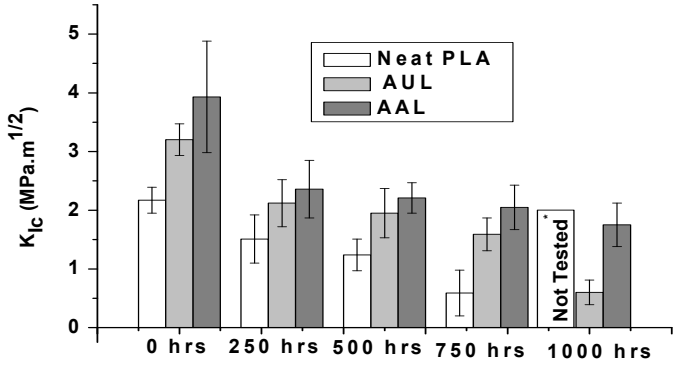

(b)

Figure 6 Effect of accelerated ageing on (a) IS and (b) K_{Ic} of neat PLA, AUL and AAL composites. Error bars each corresponds to one standard deviation.

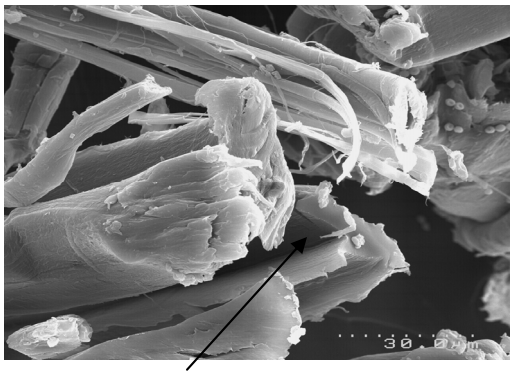

Higher loss of structural integrity

(a)

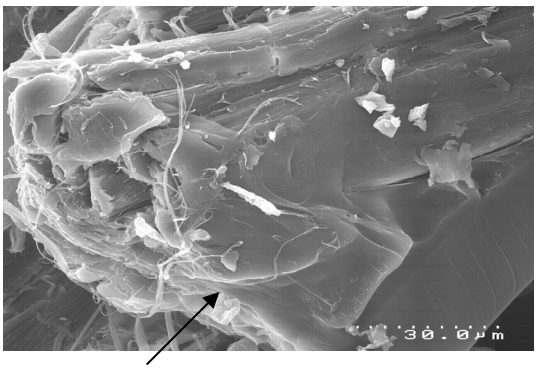

Lower loss of structural integrity

(b)

Figure 7 (a) AUL and (b) AAL composite fracture surfaces after 1000 hours accelerated ageing.

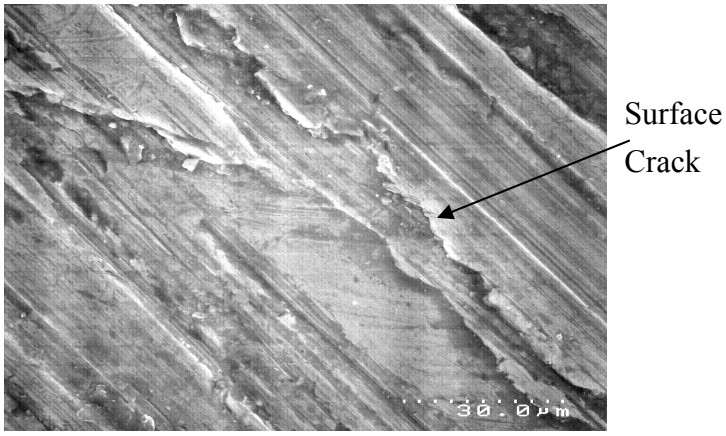

Figure 8 SEM micrograph of neat PLA surface after weathering for 750 hours.

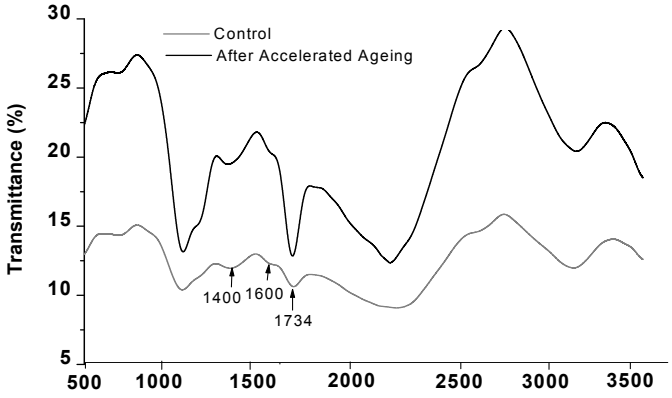

Figure 9 FTIR spectra of AUL composites.

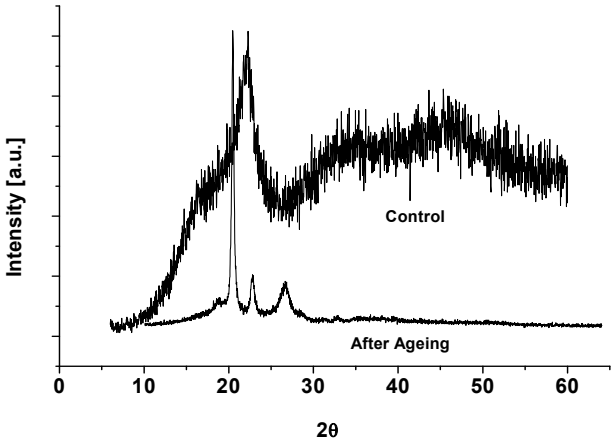

(a)

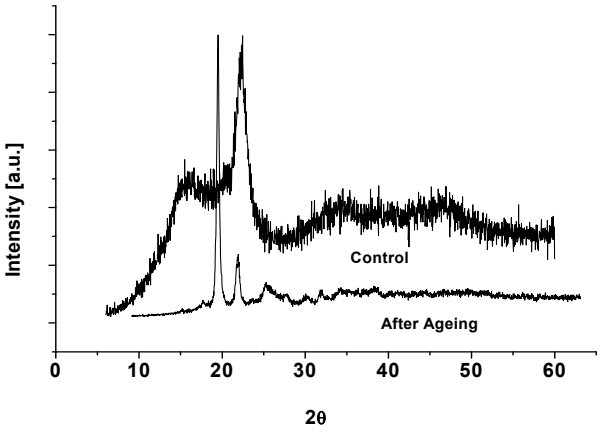

(b)

Figure 10 WAXRD pattern for (a) AUL and (b) AAL composites of control samples and after accelerated ageing of 1000 hours.

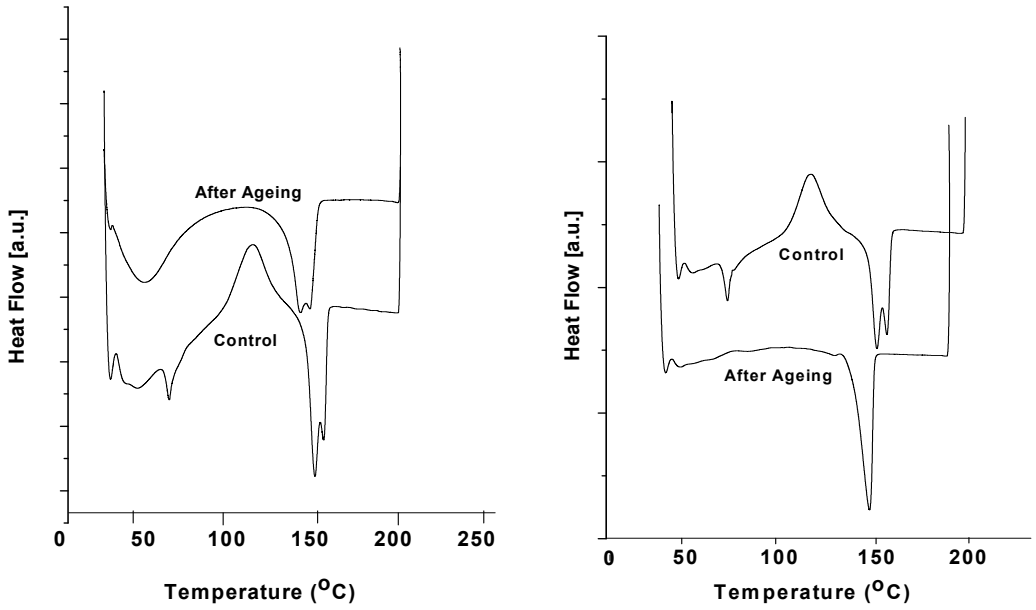

(a) **(b)**

Figure 11 DSC traces for (a) AUL and (b) AAL composites of control samples and after accelerated ageing of 1000 hours.